Crystal-Configuration Considerations for Higher-Sensitivity Picosecond-Pulse SHG FROG

Peter Šušnjar, Travis Jones, Rick Trebino, and Rok Petkovšek

***Abstract*— We experimentally compare a thick BIBO crystal, a walk-off compensating configuration of thin BBO crystals, and a thin PPLN crystal for the use as a nonlinear medium in SHG FROG, aiming for increased sensitivity required for complete pulse characterization of low-energy (below pJ) pulses a few picoseconds long at wavelengths near 1030 nm. We investigate the dependence of the spectral bandwidth of the frequency-doubled input ultrashort pulse and the conversion efficiency on focal-spot size in the nonlinear crystal. Both numerical and experimental results confirm an increase of the bandwidth with tighter focusing in a thick BIBO and a more-than-threefold increase of conversion efficiency compared to a thin BIBO crystal. A PPLN crystal is found to be the most efficient among the three, but very thin (< 0.3 mm) crystals would be required to extend the measurement capabilities of SHG FROG to sub-ps pulses. A SHG FROG using a PPLN crystal for characterization of picosecond pulse is demonstrated with a sensitivity of 2×10^{-3} (mW)^2.**

***Index Terms*— FROG, second harmonic generation, ultrashort pulse characterization.**

I. Introduction

MOST modern applications of ultrashort laser pulses require, or at least benefit from, detailed information about both its intensity and phase. Frequency-resolved optical gating (FROG) [1], [2] is the most commonly used method for accurately and reliably providing such information. Recently, it has been shown that FROG includes additional benefits, not previously realized, such as a clear indication as to whether a pulse train is stable or not [3]–[5], a highly reliable and fast pulse-retrieval algorithm [6], [7], and operation with missing data [8]. As a result, it is important to consider and potentially improve FROG's performance for pulses in all ranges.

FROG involves gating a pulse by a replica of the pulse (or another event) through a nonlinear response of a material, usually a second-harmonic-generation (SHG) crystal. The nonlinear signal is then spectrally resolved to obtain an experimental spectrogram, known as the FROG trace.

Some of the most sensitive FROG setups reported so far include SHG in a chirped, aperiodically poled lithium niobate (APPLN) waveguide [9], [10], four wave mixing (FWM) in a 22 km long dispersion-shifted fiber [11] or in a semiconductor amplifier [12], and electro-optical amplitude modulation [13]. They have all been demonstrated at telecom wavelengths (around 1550 nm) and all depend on technology not readily available at other wavelengths.

SHG, as the lowest-order nonlinear process, is particularly suitable for the characterization of weak pulses. However, it requires phase-matching and therefore has a finite bandwidth due to the dispersion of the crystal. If the entire spectrum of the measured pulse is not phase-matched, spectral filtering can occur if the crystal is too thick. Unfortunately, such thin crystals drastically reduce the SHG conversion efficiency and render traditional FROG setups incapable of measuring very weak pulses, especially for relatively long, low-energy pulses. Optimization of the SHG efficiency is therefore necessary. In this paper, we compare three possible options – a thick birefringent crystal, a walk-off compensating (WOC) stack of crystals, and a quasi-phase matched (QPM) crystal – applicable to basically any spectral range for which SHG crystals are available.

Several other experimental studies have shown efficient frequency conversion over the entire bandwidth of femtosecond pulses using SHG in a thick nonlinear crystal, when very tight focusing is employed [14]–[17]. A variant of FROG, called GRENOUILLE, also applies tight, but only one-dimensional, focusing in a very thick SHG crystal to simultaneously achieve broadband conversion and high angular spectral resolution [18]. The relevant length concerning the conversion bandwidth in birefringent crystals is actually the aperture length l_a. It is the distance after which the fundamental and second-harmonic (SH) beams separate due to spatial walk-off. On the other hand, the presence of spatial walk-off also typically reduces the efficiency of SHG. In some cases it is therefore preferable to minimize spatial walk-off, e.g. by using several thin crystals placed in a WOC configuration [19]–[21]. In this case consecutive crystals are periodically flipped for 180 degrees such that the walk-off direction is also flipped. These ideas have not yet been applied to FROG.

Another alternative is a QPM scheme with periodically poled NL crystals which offers access to very high nonlinearities. This comes at the expense of a highly dispersive

Manuscript received October 4, 2019; revised January 30, 2020; accepted January 30, 2020. Date of publication February 5, 2020; date of current version February 19, 2020. This work was supported in part by the Slovenian Research Agency under Grant P2-0270, Grant P2-0392, Grant L2-8183, Grant L2-9240, and Grant L2-9254, in part by the Strategija Pametne Specializacije (SPS) Operation entitled building blocks, tools, and systems for factories of future—GOSTOP, U.S. National Science Foundation under Grant ECCS-1609808, and in part by the Georgia Research Alliance. *(Corresponding author: Peter Šušnjar.)*

Peter Šušnjar and Rok Petkovšek are with the Faculty of Mechanical Engineering, University of Ljubljana, 1000 Ljubljana, Slovenia (e-mail: peter.susnjar@fs.uni-lj.si).

Travis Jones and Rick Trebino are with the School of Physics, Georgia Institute of Technology, Atlanta, GA 30332 USA.

Color versions of one or more of the figures in this article are available online at http://ieeexplore.ieee.org.

Digital Object Identifier 10.1109/JQE.2020.2971761

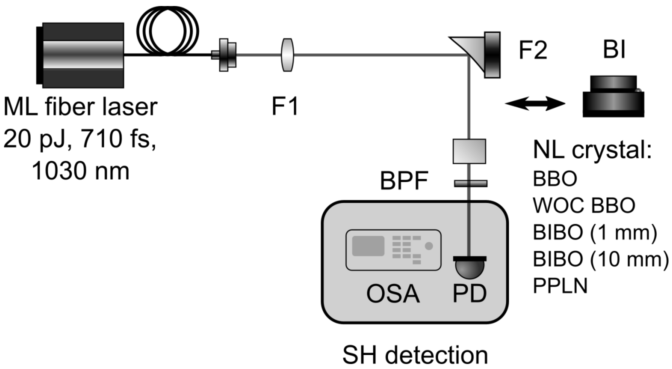

Fig. 1. The experimental setup: F1 – first lens, F2 – focusing element (off-axis parabolic mirror or lens), BI – beam profiling camera, BPF – bandpass filter, PD – power meter, OSA – spectrometer.

medium and thus again requires a very thin crystal for broadband frequency conversion. The conversion bandwidth can be increased by chirping the periods, but this comes at a cost of a non-flat spectral response and the reduced effective nonlinearity [22], [23].

The paper is organized as follows: in section II, the experimental setup for crystal comparison study is presented. The effects of focusing on conversion efficiency and conversion bandwidth for three possible alternative SHG geometries and crystals – thick BIBO, a WOC stack of BBO, and a thin PPLN, are described in sections III and IV, respectively. Additionally, experimental results are compared to theoretical predictions of Wang et al. [24] and to two numerical solvers (SNLO [25] and HUSSAR [26]). The analytical result of Wang et al. is used to derive scaling rules explicitly relevant for sensitive SHG FROG, where high conversion efficiency and broad conversion bandwidth are important, whereas beam properties can be sacrificed. Finally, the first results of a SHG FROG with the thin PPLN crystal, the most efficient among the three compared, are shown in section V demonstrating its sensitivity by measuring a 20 fJ, 7.8 ps-long pulse.

II. Experimental Setup

The experimental setup used for the comparison of nonlinear crystals is shown in Fig. 1. For experiments presented in sections III and IV, a mode-locked Yb-fiber oscillator was employed delivering pulses of 20-pJ energy at repetition rate of 27 MHz with a spectrum 3.6 nm broad and centered at 1030 nm. Its output pulses were characterized by an in-house built SHG FROG in a collinear geometry employing a 2-mm-long BBO crystal for SHG. The retrieved pulse (FROG error G = 0.0057), shown in Fig. 2, can be approximated by a linearly chirped Gaussian pulse with a pulse duration of $t_p = 0.71$ ps (FWHM value) and a linear chirp of -0.46 THz/ps.

To study the effect of focusing on conversion efficiency and conversion bandwidth, we varied the focal spot size of the beam in the SHG crystal using different combinations of a lens and a second focusing element, either an off-axis parabolic mirror or another lens. The focal spot was inspected by a beam profiling camera with a pixel size of 4.4 μm $\times$ 4.4 μm. The spot size was determined as a second moment width $D4\sigma$. For all focusing configurations, the focal spot was found to be round, with a bell-shaped cross-section and parabolic caustics. It can therefore be well approximated by a single mode Gaussian beam with a beam waist w_0 spanning from 6 to 100 μm. For the tightest focusing, however, the beam only filled a few pixels and so resulted in the retrieved beam diameter for the tightest focus having a large measurement uncertainty.

The SHG crystals used in this study were a 2-mm-long BBO, a WOC stack of four 0.5-mm-long BBO crystals, a 1- and 10-mm-long BIBO and a 1-mm-long PPLN chip with 5 channels with different poling periods from 6.16 to 6.29 μm. Both BBO and BIBO crystals were cut for type-I phase matching (ooe and eeo, respectively), whereas type-0 (eee) quasi phase matching (QPM) was employed for SHG in PPLN. The BBO crystals and the PPLN chip had a dual-band AR coating on the front and rear surfaces for the fundamental and second harmonic (SH) light, while the BIBO crystals were uncoated. The WOC stack consisted of two pairs of bonded BBO crystals placed in WOC configuration. As the crystal manufacturer could only bond 2 crystals together, we placed the two pairs together in a holder using a thin layer of foil as a spacer to avoid surface damage with a clearance for beam to pass through. Prior to that, we had determined the correct relative orientation between the pairs by measuring the SH power for all possible orientations as well as for each pair alone. While there are two possible walk-off compensating orientations, for one there is also a change of sign of effective nonlinearity equivalent to a phase shift of π [27]. The one that yielded the highest conversion efficiency was selected for further analysis. The PPLN chip was placed in an oven and was heated to temperatures ranging from 35 °C to 42 °C. The temperature was varied to find an optimal phase mismatch for a given focusing situation, with a peak of SH spectrum matching the corresponding peak of the fundamental one. The crystals were mounted such that all 6 degrees of freedom (rotational and translational) could be optimized. A bandpass filter was placed behind the NL crystal transmitting only the SH light at 515±5 nm. The SH power was measured by a power meter placed behind the filter whose transmittance was pre-calibrated. After optimizing the conversion efficiency, the SH light was coupled into a multimode fiber and guided to a slitless spectrometer employing the fiber output as an input slit. To get rid of the modal interference pattern, the coupling fiber was mechanically scrambled [28]. Spectra were acquired by averaging over several periods of the fiber scrambler. In some cases however, residual distortions in the spectrum remained.

III. Conversion Efficiency of SHG With Ultrashort Pulses

The highest possible efficiency of the nonlinear process used for optical gating in FROG measurements is crucial for the characterization of weak pulses. The efficiency of SHG, our nonlinear gating process of choice, depends both on the properties of the nonlinear crystal and on the generation conditions such as focusing and phase mismatch.

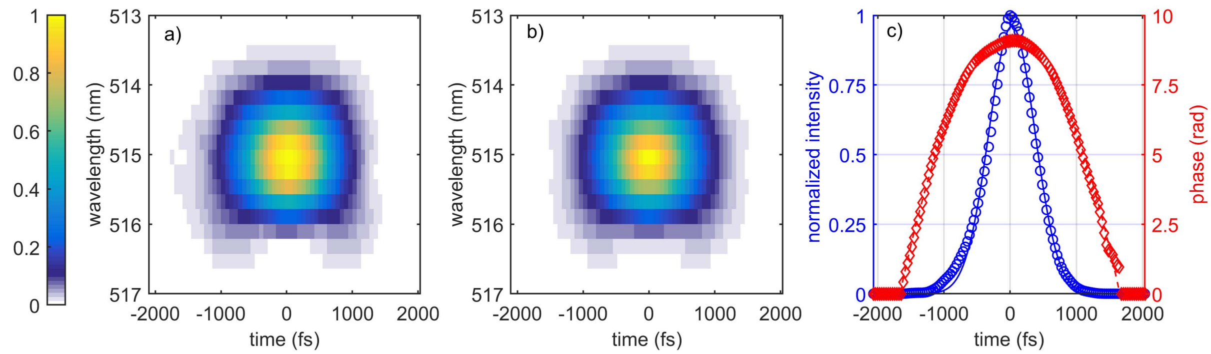

Fig. 2. a,b) SHG FROG trace (measured and retrieved) of a pulse used for SHG experiments. c) Retrieved pulse shape – intensity and phase in time domain with a Gaussian and parabolic fit respectively.

TABLE I
RELEVANT CRYSTAL PARAMETERS FOR SHG WITH ULTRASHORT PULSES FOR NONLINEAR CRYSTALS USED IN OUR EXPERIMENTAL STUDY

	BBO		BIBO		PPLN
Crystal length – *L* [mm]	2	4x0.5	1	10	1
Effective nonlinear coefficient d_{eff} [pm/V]	2.01		3.40		16.0
Temporal walk-off – *GVM* x *L* [fs]	187	187	193	1930	896
Walk-off angle - ρ [mrad]	57	~14	30.5	30.5	no

SHG with ultrashort pulses has been studied by many authors, both analytically and numerically [24], [29], [30] under different approximations. For a quick analysis of optimal generation condition relevant for SHG FROG with a thick SHG crystal we can proceed with a simple asymptotic result of Wang and Weiner for conversion efficiency [24]

$$\eta_a \propto \frac{d_{eff}^2 l_{S\text{-}T}}{t_p} \tan^{-1}\left(\frac{L}{b}\right), \tag{1}$$

which holds for the case of strong walk-off ($l_{S-T} \ll b,\ L$), zero phase mismatch, and a focus in the center of the crystal. Here, d_{eff} is an effective nonlinear coefficient, t_p is a FWHM-pulse duration, b is a confocal parameter of a Gaussian beam and l_{S-T} is the generalized walk-off length that equals

$$l_{S\text{-}T} = \left(\frac{\rho^2}{w_0^2} + \frac{(\alpha^2+16)GVM^2 \ln 2}{8t_p^2}\right)^{-1/2} \tag{2}$$

with ρ, α and *GVM* being a spatial walk-off angle, a dimensionless chirp parameter [24] and a group velocity mismatch, respectively.

By using (1) one should proceed in the following way to determine the optimal SHG conditions. First, the beam should be focused tightly for broadband up-conversion (for the exact criterion see the next section). Consequently, spatial-walk-off would typically prevail over temporal walk-off so that aperture length, $l_a = w_0/\tan(\rho) \approx w_0/\rho$, should be used in place of l_{S-T}. Then, for the longest allowed l_a, one can easily check, how much the conversion efficiency improves when using a longer crystal and can select a crystal length accordingly. As a rule of thumb, for a ratio $L/b \approx 4$, η_a is already at 85 % of the maximal value (for infinitely long crystal). Above that point, increasing the crystal length would no longer significantly improve conversion efficiency. As evident from (1), conversion efficiency can be also increased by introducing a longer aperture length, not by focusing more loosely however, but by reducing the walk-off angle. At the same time, the overall temporal stretch $GVM \times l_a$ should still be kept below the pulse coherence time. One way to do that is by placing several thin nonlinear crystals in a walk-off compensating direction, so that the fundamental and SH beams do not or only partially walk away. Theoretical studies have shown [20], [31] that a segment of N nonlinear crystals in a WOC geometry can improve conversion efficiency by almost a factor of N compared to a single crystal. As it was suggested by [32], we can approximate the effective walk-off angle as $\rho_{eff} = \rho/N$ and use this in numerical simulations as an approximation. Full simulation using a numerical solver, HUSSAR [26], confirmed the validity of such approximation (see Fig. 3b).

We have experimentally investigated the optimal focusing condition in terms of conversion efficiency for all possible improvements, i.e., thick birefringent crystal (Fig. 3a), WOC geometry (Fig. 3b), and a QPM scheme with a PPLN crystal (Fig. 3c). Our measurements were also compared with the theoretical model of Wang and Weiner [24] and numerical solvers SNLO (2D-mix-SP) and HUSSAR. The dependence of conversion efficiency upon focusing resembles the theoretical predictions, with a perfect agreement on optimal focal spot size for all crystals but the WOC stack of BBOs. However, the measured absolute conversion efficiencies for BBO and BIBO crystals are around 60 % of the predicted ones (at maximal values it is 67 %, 57 % and 59 % for 2-mm BBO, 1-mm BIBO and 10-mm BIBO, respectively). The conversion is improved by a factor of 3.4 for the thicker BIBO compared to the thinner one. The aperture length for this optimal focusing ($D_{FWHM} = 27\mu$m) equals $l_a = 750\mu$m, corresponding to a temporal walk-off of 140 fs, which roughly determines the shortest pulse to be measured by SHG FROG in such a geometry.

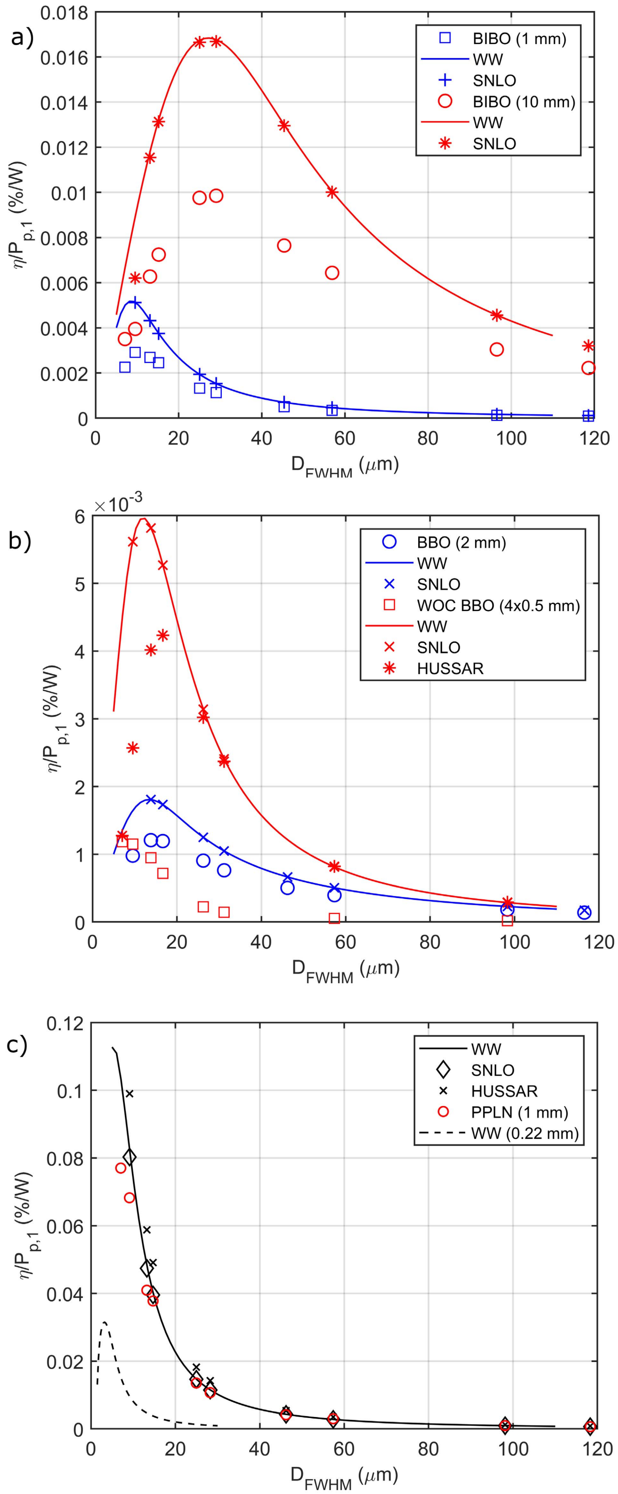

Fig. 3. Conversion efficiency in units %/peak power vs focal spot size for: a) thick (10 mm) and thin (1 mm) BIBO crystals, b) walk-off compensated stack and a single BBO crystal, and c) a 1 mm long PPLN. Experimental values (circles and squares) are compared with theoretical predictions of Wang and Weiner's (WW) model (eq. 19 in the ref. [24]) and full numerical solvers SNLO and HUSSAR. A simulation result for a 0.22 mm thick PPLN crystal with the same temporal walk-off as 2 mm BBO is also shown.

In the case of the WOC configuration, we have witnessed a rather different behavior than predicted by the theoretical model with adjusted walk-off angle and by full simulation with numerical solver HUSSAR, where the exact geometry with crystal flips can be simulated. On one hand we could observe the effective mitigation of the spatial walk-off effect as an increase in the acceptance angle manifested as a rounder beam profile compared to a single BBO crystal. Yet, the conversion efficiency was only 20-30 % of the predicted one. The optimal focusing also shifted to very small focal spots ($D_{\mathrm{FWHM}} = 6\mu$m) sembling a behavior expected for much a thinner crystal than the one used. We have observed the same discrepancy between the numerical models and the measured SH power also for a single pair. While we cannot make a definite claim, we suspect that either misalignment, stress or even wrong relative orientation within the pair was introduced at the time of bonding. Additional phase mismatch could also arise from AR coatings and misalignment when the pairs were put together in their holders. Nevertheless, we should stress that, at least in theory (see Fig. 3b), a WOC geometry should lead to a similar improvement (factor of 3.3) as a thick NL crystal. However, this seems to be technically far more challenging to implement, whereas full commercial WOC solutions are available only for certain nonlinear crystals.

The highest conversion efficiency was reached with the 1-mm-long PPLN crystal, which was in a perfect agreement with theoretical predictions. However, a 900-fs-long temporal walk-off at 1030 nm makes this crystal unsuitable for characterization of pulses with temporal structures shorter than few picoseconds. A PPLN crystal with the same conversion bandwidth (and temporal walk-off) as a 2-mm-thick BBO would have to be only 0.22 mm long. The conversion efficiency for that case was calculated by Wang and Weiner's analytical result and is shown in Fig. 3c by a dashed line. The highest possible conversion is still 1.87-times higher than for the thick BIBO, but it is reached only at extremely tight focusing to a spot of $D_{\mathrm{FWHM}} = 3\mu$m and then quickly falls with looser focusing.

IV. Spectral Bandwidth of Up-Converted Ultrashort Pulse

For SHG FROG to measure the right pulse shape, the entire spectrum of the pulse must be efficiently up-converted [2]. If not, the retrieved pulse would typically be shorter than the real one, similarly as is the case in an autocorrelation measurement [33]. We measured the SH spectral bandwidth of an up-converted ultrashort pulse for all SHG crystals in this study to prove their applicability for SHG FROG. Next, we studied the effect of focusing on the spectral bandwidth for a birefringent crystal in the presence of spatial walk-off. Using a plane wave description, we found a simple criterion for focusing to ensure the complete spectral up-conversion of a given spectral bandwidth.

The measured spectra for the case of the tightest focusing are shown in Fig. 4. The spectral width is approximately the same for all birefringent crystals and significantly narrower for the PPLN due to its narrower phase matching bandwidth, which cannot be increased by tighter focusing as is the case for NCPM in birefringent crystals. The spectrum retrieved by the full numerical simulation with the SNLO software for the SHG in a 2-mm-thick BBO crystal is also shown for comparison

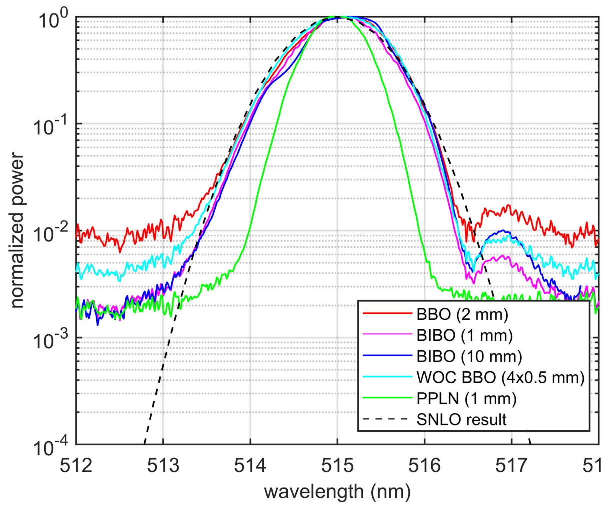

Fig. 4. SH spectra for SHG in all crystals and the tightest focusing utilized. A result of numerical simulation (dashed line) is plotted for comparison.

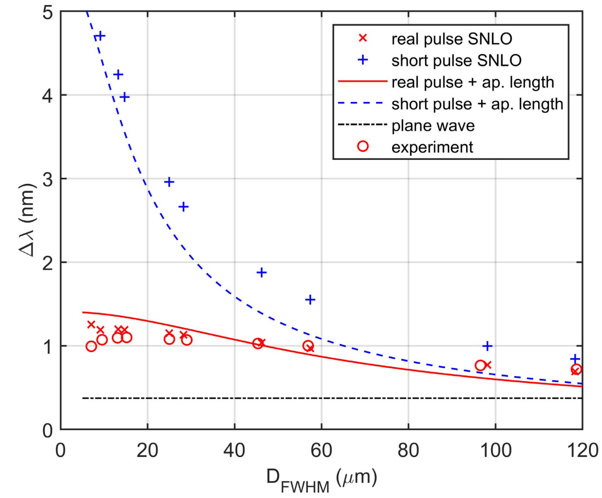

Fig. 5. FWHM bandwidth of SH spectrum vs focal spot for SHG in a 10 mm thick BIBO for a measured, 710 fs pulse and also theoretical predictions only for a shorter (100 fs, bandwidth-limited Gaussian) pulse.

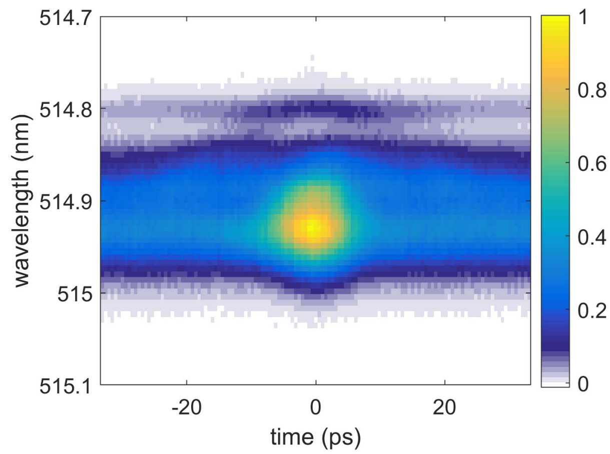

Fig. 6. Measured FROG trace of a 20 fJ pulse before trace processing - background subtraction and low-pass Fourier filtering.

(dashed line). The experimental bandwidths agree well with the theoretical bandwidth from SNLO.

In general, the main reason for spectral filtering is the non-zero phase mismatch between nonlinear polarization and second harmonic (SH) field at frequencies away from the central (phase-matched) frequency. The spectral filter for the plane wave in the SHG has a form [33]

$$F(\omega) = \frac{\sin\frac{\Delta k(\omega)L}{2}}{\frac{\Delta k(\omega)L}{2}} \tag{3}$$

Here, L is the crystal length, while phase mismatch for the collinear SHG geometry can be written in general as [34]

$$\Delta k(\omega,\theta) = k_o(2\omega) - 2k_e(\omega,\theta)\ , \tag{4}$$

where θ is the angle between the beam propagation direction and the optical axis of a birefringent NL crystal, and k_o and k_e are the wavenumbers of the ordinary and extraordinary polarized electric fields, respectively. We assume type-I phase matching with ordinary polarized SH and extraordinary polarized fundamental field, as is the case for the SHG in BIBO at 1030 nm.

The phase mismatch is exactly zero at a single frequency-angle pair, e.g., at the angle θ_0 for the central frequency ω_0, while the conversion is still efficient within the phase matching bandwidth $\Delta\omega_{PM}$ commonly defined as $\Delta k(\omega_0 \pm \Delta\omega_{PM}/2)L/2 = \pi$. However, by focusing tightly into the crystal, the angular spread of a beam can be sufficient enough to compensate for the dispersion. Expanding (4) around (ω_0,θ_0) to the first order yields the condition for the required beam divergence

$$\Delta\theta = -\frac{\partial \Delta k}{\partial \omega} \Bigg/ \frac{\partial \Delta k}{\partial \theta}\Delta\omega \tag{5}$$

The partial derivatives can be related to known crystal parameters, namely to the walk-off angle ρ, given by $\tan(\rho) = -n_e^{-1}(\partial n_e\ /\partial\theta)$, where n_e is an extraordinary refractive index, and to the group velocity $v_g = (\partial k/\partial\omega)^{-1}$. A zeroth-order Gaussian beam with a full beam divergence $\Delta\theta = 2\lambda_0/(\pi n w_0)$ should be therefore focused to a beam waist smaller than

$$w_0 < \frac{4\tan(\rho)}{GVM\,\Delta\omega} \tag{6}$$

in order to completely frequency-double a spectrum with a spectral width $\Delta\omega$, where $GVM = 1/v_{g,2} - 1/v_{g,1}$ is the group velocity mismatch between the fundamental and the SH frequency.

Spectral filtering can also be understood in a real-space representation of the SHG with ultrashort pulses. Due to the different group velocities of the fundamental and the SH pulse, the up-converted pulse stretches as the part generated at the beginning of the crystal lags behind the part generated at the end of the crystal. This effect is known as a temporal walk-off. However, in the presence of a spatial walk-off, the beams also separate within one aperture length l_a. The temporal stretch therefore equals *GVM* x l_a. It can be made small compared to the pulse coherence time $\tau_c \approx 2\pi/\Delta\omega$ by tight focusing to a focal spot

$$w_0 < \frac{\tan(\rho)}{GVM}\tau_c, \tag{7}$$

which is up to a constant the same criterion as (6).

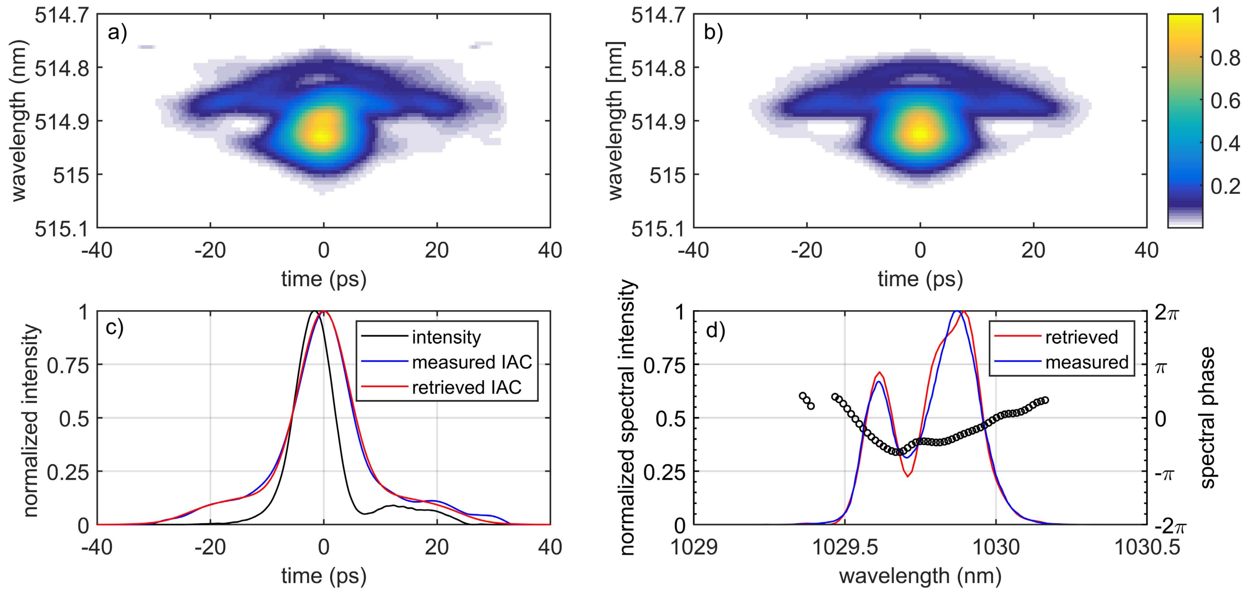

Fig. 7. SHG FROG measurement of an internally-built mode-locked fiber oscillator: a) measured FROG trace, b) retrieved FROG trace (error G = 0.0084), c) retrieved temporal intensity and autocorrelation (IAC), and d) spectral intensities (measured and retrieved) and phase (circles).

In the case of QPM geometry, all interacting waves are polarized along the optical axis so that there is no angular dispersion of the refractive index in the first order and therefore no spatial walk-off. The interaction length is set by the shortest among the crystal length or the confocal parameter of the focused beam. The latter is still relatively long for even the tightest focusing condition tested. Relatively large temporal walk-off and correspondingly narrow spectral bandwidth could therefore not be avoided for this crystal length.

To experimentally prove the possibility of compensation of phase-mismatch by tight focusing, we have investigated the conversion bandwidth dependence on focal spot size for SHG in a 10-mm-BIBO crystal. We found good agreement between our experimental results of FWHM bandwidth of SH spectra and SNLO (see Fig. 5, full line, circles), confirming that the conversion bandwidth can be increased by a tighter focusing. A very similar trend can be seen from a simple approximation shown by the full line where spectral filtering was calculated using (3) with aperture length l_a instead of a full crystal length. As our pulse has a relatively narrow bandwidth, it is difficult to evaluate the accuracy of this approximation. To account for this limitation, we also simulated SHG in a 10-mm-BIBO for a 100-fs long bandwidth-limited Gaussian pulse (dashed line). Our approximation accurately predicts the conversion bandwidth for tight focusing and slightly underestimates it for loose focusing. In any case, our prediction is still much more accurate than the simple plane wave approximation, which neglects the focusing and the spatial walk-off effects (dashed-dot line). For this reason, we suggest the aperture length as a relevant dimension when estimating the phase-matching bandwidth for NCPM SHG from temporal walk-off ($GVM \times L$) or rules (6) or (7) when one is choosing the right focusing.

V. Test of a Highly Sensitive SHG FROG Using a PPLN Crystal

For our highly sensitive SHG FROG we chose a PPLN crystal as it proved to be the best nonlinear crystal in terms of conversion efficiency among compared. A collinear geometry was applied with a pulse and its delayed replica propagating along the same path. The SHG is more efficient in that way, because the tightly focused beams fully overlap within the entire length of the crystal. The collinear geometry also allowed us to use the same, standard PPLN crystal with a period of 6.26 μm, optimal for SHG around 1030 nm, while we would need a custom one to achieve QPM in a non-collinear geometry. We washed out interferometric fringes between a pulse and its replica to the level of noise by dithering a mirror in one arm of the Michelson interferometer used for generation of delayed replica. The mirror was mounted on a linear translation stage with a piezo actuator that was driven by a triangular voltage signal with a frequency of 20 Hz. The amplitude of the signal was precisely chosen, such that the stage would move over exactly two interferometric fringes. Guided by our previous tests on conversion efficiency, we tightly focused the beam into a crystal to a focal spot of about 5 μm. The focal spot served as an entrance slit of a spectrometer, which was built right after the crystal. In addition to high SHG conversion efficiency, this is an important contribution to increased sensitivity of this FROG system as no signal light is lost due to coupling in a spectrometer. Spherical mirrors with 250-mm and 500-mm focal lengths were used for re-collimation and focusing, and a 25-mm-wide reflective diffraction grating with a ruling of 1800 lines/mm was used for dispersing a SH light. They were placed in an asymmetric Czerny-Turner geometry with angles optimized for minimal aberrations. The SH light was detected by a standard monochromatic CMOS industrial camera.

The spectrometer was calibrated with a double pulse with a known delay between the pulses. A spectral fringe depth above 60 % was achieved for the delay of 27 ps giving a rough approximation of spectral resolution of 33 pm.

We performed an SHG FROG measurement of an in-house built SESAM-mode locked fiber oscillator with a central wavelength of 1029.8 nm and a repetition rate of 37 MHz. The FROG trace shown in Fig. 6 was recorded with an average power of 750 nW, corresponding to a pulse energy of 20 fJ. With an integration time of the camera set to 1 s, the measurement took about 3 minutes. The delay marginal of the measured FROG trace had a ratio of background vs. peak of 1:2.96, very close to the expected 1:3 (for an intensity autocorrelation with background to which it corresponds). We also evaluated the presence of background noise from the edges of the trace to be 1/568 of the peak value at zero delay.

To prepare the trace for retrieval, we subtracted the DC background which was calculated as an average over the first and the last five delay points. After that, a mild high frequency noise Fourier filtering was performed to yield a trace shown in Fig. 7a. For the retrieval we used the RANA algorithm [7]. A low G error of 0.0084 and a good agreement between the retrieved and measured spectrum of the pulse (see Fig. 7d) confirm the successful retrieval of a 7.6-ps-long pulse with an accompanying, weak satellite pulse(s). A sensitivity of the SHG FROG setup given in terms of product of average and peak power of the weakest detectable pulse can be therefore estimated to 2×10^{-3} $(\mathrm{mW})^2$.

VI. Conclusion

We have investigated three possible SHG geometries and crystals – a thick birefringent crystal BIBO, a walk-off compensating configuration of BBO crystals, and QPM in PPLN, to be used in a SHG FROG with improved sensitivity for characterization of low energy pulses in the picosecond range. We have studied the dependence of the conversion bandwidth on focusing in a 10-mm-thick BIBO and confirmed that it can be significantly increased (compared to a plane wave limit) by the tight focusing. For that case, the aperture length is found to be the relevant length for spectral filtering due to finite phase-matching bandwidth. We confirmed this approximation by the numerical solver SNLO also for a shorter, 100 fs pulse. The experimentally found optimal focusing is in agreement with the analytical result of Wang and Weiner [24] for all crystals, except for the walk-off compensating configuration. An improvement in conversion efficiency by a factor of 3.4 was measured for the thick BIBO compared to the thin one. SHG is the most efficient in a PPLN, yet a more than 4-times shorter crystal (0.22 mm) would be required to convert a spectrum as broad as the other crystals can. Apart from SHG FROG, here presented results can also serve as a guideline for the selection of NL crystal and focusing for SHG with ultrashort pulses when an efficient conversion of a broad spectrum is of the main concern. Finally, using all of the above, we built an SHG FROG with a PPLN crystal and demonstrated its capability to fully characterize sub-pJ, few-ps pulses.

References

[1] R. Trebino *et al.*, "Measuring ultrashort laser pulses in the time-frequency domain using frequency-resolved optical gating," *Rev. Sci. Instrum.*, vol. 68, no. 9, pp. 3277–3295, Sep. 1997.

[2] R. Trebino, *Frequency-Resolved Optical Gating: The Measurement of Ultrashort Laser Pulses*. New York, NY, USA: Springer, 2002.

[3] M. Rhodes, Z. Guang, and R. Trebino, "Unstable and multiple pulsing can be invisible to ultrashort pulse measurement techniques," *Appl. Sci.*, vol. 7, no. 1, p. 40, Dec. 2016.

[4] M. Rhodes, G. Steinmeyer, J. Ratner, and R. Trebino, "Pulse-shape instabilities and their measurement," *Laser Photon. Rev.*, vol. 7, no. 4, pp. 557–565, Jul. 2013.

[5] J. Ratner, G. Steinmeyer, T. C. Wong, R. Bartels, and R. Trebino, "Coherent artifact in modern pulse measurements," *Opt. Lett.*, vol. 37, no. 14, pp. 2874–2876, Jul. 2012.

[6] R. Jafari and R. Trebino, "Highly reliable frequency-resolved optical gating pulse-retrieval algorithmic approach," *IEEE J. Quantum Electron.*, vol. 55, no. 4, pp. 1–7, Aug. 2019.

[7] R. Jafari, T. Jones, and R. Trebino, "100% reliable algorithm for second-harmonic-generation frequency-resolved optical gating," *Opt. Express*, vol. 27, no. 3, pp. 2112–2124, Feb. 2019.

[8] P. Sidorenko, O. Lahav, Z. Avnat, and O. Cohen, "Ptychographic reconstruction algorithm for frequency-resolved optical gating: Super-resolution and supreme robustness," *Optica*, vol. 3, no. 12, pp. 1320–1330, Dec. 2016, doi: 10.1364/optica.3.001320.

[9] S.-D. Yang, A. M. Weiner, K. R. Parameswaran, and M. M. Fejer, "Ultrasensitive second-harmonic generation frequency-resolved optical gating by aperiodically poled $LiNbO_3$ waveguides at 1.5 μm," *Opt. Lett.*, vol. 30, no. 16, pp. 2164–2166, 2005.

[10] H. Miao, A. M. Weiner, C. Langrock, R. V. Roussev, and M. M. Fejer, "Polarization-insensitive ultralow-power second-harmonic generation frequency-resolved optical gating," *Opt. Lett.*, vol. 32, no. 7, pp. 874–876, Apr. 2007.

[11] P.-A. Lacourt, J. M. Dudley, J.-M. Merolla, H. Porte, J.-P. Goedgebuer, and W. T. Rhodes, "Milliwatt-peak-power pulse characterization at 1.55 μm by wavelength-conversion frequency-resolved optical gating," *Opt. Lett.*, vol. 27, no. 10, pp. 863–865, 2002.

[12] P.-A. Lacourt, M. Hanna, and J. Dudley, "Broad-band and ultrasensitive pulse characterization using frequency-resolved optical gating via four-wave mixing in a semiconductor optical amplifier," *IEEE Photon. Technol. Lett.*, vol. 17, no. 1, pp. 157–159, Jan. 2005, doi: 10.1109/lpt.2004.837743.

[13] C. Dorrer and I. Kang, "Simultaneous temporal characterization of telecommunication optical pulses and modulators by use of spectrograms," *Opt. Lett.*, vol. 27, no. 15, p. 1315, Aug. 2002, doi: 10.1364/ol.27.001315.

[14] N. A. Chaitanya, A. Aadhi, R. P. Singh, and G. K. Samanta, "Type-I frequency-doubling characteristics of high-power, ultrafast fiber laser in thick BIBO crystal," *Opt. Lett.*, vol. 39, no. 18, p. 5419, Sep. 2014, doi: 10.1364/ol.39.005419.

[15] M. Ghotbi and M. Ebrahim-Zadeh, "Optical second harmonic generation properties of BiB_3O_6," *Opt. Express*, vol. 12, no. 24, p. 6002, Dec. 2004, doi: 10.1364/opex.12.006002.

[16] N. A. Chaitanya, A. Aadhi, S. C. Kumar, M. V. Jabir, G. K. Samanta, and M. Ebrahim-Zadeh, "Frequency-doubling of femtosecond pulses in 'thick' nonlinear crystals with different temporal and spatial walk-off parameters," *IEEE Photon. J.*, vol. 8, no. 6, Dec. 2016, Art. no. 6100613, doi: 10.1109/jphot.2016.2626198.

[17] A. M. Weiner, A. M. Kan'an, and D. E. Leaird, "High-efficiency blue generation by frequency doubling of femtosecond pulses in a thick nonlinear crystal," *Opt. Lett.*, vol. 23, no. 18, pp. 1441–1443, Sep. 1998.

[18] P. O'Shea, M. Kimmel, X. Gu, and R. Trebino, "Highly simplified device for ultrashort-pulse measurement," *Opt. Lett.*, vol. 26, no. 12, pp. 932–934, Jun. 2001.

[19] K. Hara, S. Matsumoto, T. Onda, W. Nagashima, and I. Shoji, "Efficient ultraviolet second-harmonic generation from a walk-off-compensating β-BaB_2O_4 device with a new structure fabricated by room-temperature bonding," *Appl. Phys. Express*, vol. 5, no. 5, May 2012, Art. no. 052201, doi: 10.1143/APEX.5.052201.

[20] J.-J. Zondy, D. Kolker, C. Bonnin, and D. Lupinski, "Second-harmonic generation with monolithic walk-off-compensating periodic structures II experiments," *J. Opt. Soc. Amer. B, Opt. Phys.*, vol. 20, no. 8, pp. 1695–1707, Aug. 2003, doi: 10.1364/josab.20.001695.

[21] R. J. Gehr, M. W. Kimmel, and A. V. Smith, "Simultaneous spatial and temporal walk-off compensation in frequency-doubling femtosecond pulses in β-BaB_2O_4," *Opt. Lett.*, vol. 23, no. 16, pp. 1298–1300, 1998.

[22] G. Imeshev, M. A. Arbore, M. M. Fejer, A. Galvanauskas, M. Fermann, and D. Harter, "Ultrashort-pulse second-harmonic generation with longitudinally nonuniform quasi-phase-matching gratings: Pulse compression and shaping," *J. Opt. Soc. Amer. B, Opt. Phys.*, vol. 17, no. 2, pp. 304–318, Feb. 2000.

[23] A. M. Schober, M. Charbonneau-Lefort, and M. M. Fejer, "Broadband quasi-phase-matched second-harmonic generation of ultrashort optical pulses with spectral angular dispersion," *J. Opt. Soc. Amer. B, Opt. Phys.*, vol. 22, no. 8, pp. 1699–1713, Aug. 2005.

[24] H. Wang and A. Weiner, "Efficiency of short-pulse type-i second-harmonic generation with simultaneous spatial walk-off, temporal walk-off, and pump depletion," *IEEE J. Quantum Electron.*, vol. 39, no. 12, pp. 1600–1618, Dec. 2003, doi: 10.1109/jqe.2003.819531.

[25] *MATLAB SNLO*. Accessed: Jan. 11, 2019. [Online]. Available: http://www.as-photonics.com/products/matlab-snlo

[26] T. M. Kardaś, M. Nejbauer, P. Wnuk, B. Resan, C. Radzewicz, and P. Wasylczyk, "Full 3D modelling of pulse propagation enables efficient nonlinear frequency conversion with low energy laser pulses in a single-element tripler," *Sci. Rep.*, vol. 7, Feb. 2017, Art. no. 42889, doi: 10.1038/srep42889.

[27] D. J. Armstrong, W. J. Alford, T. D. Raymond, A. V. Smith, and M. S. Bowers, "Parametric amplification and oscillation with walkoff-compensating crystals," *J. Opt. Soc. Amer. B, Opt. Phys.*, vol. 14, no. 2, p. 460, Feb. 1997, doi: 10.1364/josab.14.000460.

[28] R. R. Petersburg *et al.*, "Modal noise mitigation through fiber agitation for fiber-fed radial velocity spectrographs," *Astrophys. J.*, vol. 853, no. 2, p. 181, Feb. 2018, doi: 10.3847/1538-4357/aaa487.

[29] E. Sidick, A. Knoesen, and A. Dienes, "Ultrashort-pulse second-harmonic generation. I. Transform-limited fundamental pulses," *J. Opt. Soc. Amer. B, Opt. Phys.*, vol. 12, no. 9, pp. 1704–1712, Sep. 1995, doi: 10.1364/JOSAB.12.001704.

[30] S. M. Saltiel, K. Koynov, B. Agate, and W. Sibbett, "Second-harmonic generation with focused beams under conditions of large group-velocity mismatch," *J. Opt. Soc. Amer. B, Opt. Phys.*, vol. 21, no. 3, p. 591, Mar. 2004, doi: 10.1364/josab.21.000591.

[31] A. V. Smith, D. J. Armstrong, and W. J. Alford, "Increased acceptance bandwidths in optical frequency conversion by use of multiple walk-off-compensating nonlinear crystals," *J. Opt. Soc. Amer. B, Opt. Phys.*, vol. 15, no. 1, pp. 122–141, Jan. 1998.

[32] J.-J. Zondy, C. Bonnin, and D. Lupinski, "Second-harmonic generation with monolithic walk-off-compensating periodic structures. I. Theory," *J. Opt. Soc. Amer. B, Opt. Phys.*, vol. 20, no. 8, pp. 1675–1694, Aug. 2003, doi: 10.1364/josab.20.001675.

[33] A. Weiner, "Effect of group velocity mismatch on the measurement of ultrashort optical pulses via second harmonic generation," *IEEE J. Quantum Electron.*, vol. QE-19, no. 8, pp. 1276–1283, Aug. 1983.

[34] A. V. Smith, *Crystal Nonlinear Optics: With SNLO Examples*. Albuquerque, NM, USA: AS-Photonics, 2015.

Peter Šušnjar was born in Kranj, Slovenia, in 1990. He received the B.S. and M.S. degrees in physics from the University of Ljubljana, Ljubljana, Slovenia, in 2012 and 2016, respectively, where he is currently pursuing the Ph.D. degree in physics.

He worked as a Visiting Master Student at the Laser Spectroscopy Division, Max-Planck-Institute for Quantum Optics, in 2015. In the Summer of 2016, he did an internship at the Max-Born-Institute. Since Fall 2016, he has been employed at the Faculty of Mechanical Engineering, University of Ljubljana. His main areas of research interests include ultrafast and nonlinear optics, especially characterization of low-energy ultrashort pulses.

Travis Jones was born in Fairfax, Virginia, in 1993. He received the B.S. degree in physics from Wake Forest University, Winston Salem, NC, USA, in 2014, and the M.S. degree in physics from the Georgia Institute of Technology, Atlanta, GA, USA, in 2017, where he is currently pursuing the Ph.D. degree with the School of Physics, under the supervision of Prof. R. Trebino.

Rick Trebino was born in Boston, MA, USA, in 1954. He received the B.A. degree from Harvard University in 1977, and the Ph.D. degree from Stanford University in 1983.

His dissertation research involved the development of a technique for the measurement of ultrafast events in the frequency domain using long-pulse lasers by creating moving gratings. He continued this research during a three-year term as a Physical Sciences Research Associate at Stanford. In 1986, he moved to Sandia National Laboratories, Livermore, CA, USA, where he studied higher-order wave-mixing, nonlinear-optical perturbation theory using Feynman diagrams, and ultrashort-laser-pulse techniques with application to chemical dynamics measurements and combustion diagnostics, where he developed Frequency-Resolved Optical Gating (FROG), the first technique for the measurement of the intensity and phase of arbitrary ultrashort laser pulses. In 1998, he became the Georgia Research Alliance-Eminent Scholar Chair of Ultrafast Optical Physics at the Georgia Institute of Technology, Atlanta, GA, USA, where he currently researches ultrafast optics and applications.

Prof. Trebino is a fellow of the Optical Society of America, the American Physical Society, the American Association for the Advancement of Science, and the Society of Photo-Instrumentation Engineers. He has received numerous prizes, including the SPIE's Edgerton Prize and an R&D 100 Award, and he was an IEEE Lasers and Electro-Optics Society Distinguished Lecturer. He also recently won the SPIE's Yzuel Award for his pioneering contributions to optics education.

Rok Petkovšek was born in Ljubljana, Slovenia, in 1969. He received the B.S. and M.S. degrees in physics and the Ph.D. degree from the University of Ljubljana, Ljubljana, in 1994, 1999, and 2003, respectively.

From 1995 to 2003, he worked as a Researcher at the Jozef-Stefan-Institute. In 2003, he joined the Faculty of Mechanical Engineering, University of Ljubljana, as a Senior Researcher, where he founded a new laboratory for photonics and laser systems in 2016, and has served as its Head ever since. Since 2016, he has also been the Chair of the Department of Optodynamics and Laser Technology, Faculty of Mechanical Engineering, University of Ljubljana. He has published more than 50 peer-reviewed journal articles. His research interests include development of new laser sources and their application for industry and medicine.